

Maximising the Average Spectral Efficiency of Dual-Branch MIMO Systems with Discrete Rate Adaptation

Sébastien de la Kethulle de Ryhove and Geir E. Øien
 Norwegian University of Science and Technology
 Dept. of Electronics and Telecommunications
 O.S. Bragstads plass 2B, N-7491 Trondheim, Norway
 Tel: +47-73594315. Email: {delaketh, oien}@iet.ntnu.no

Abstract—The capacity of MIMO systems with perfect transmitter and receiver channel state information (CSI) can be attained by decoupling the MIMO channel into a set of independent subchannels, and distributing the power among these subchannels in accordance with the *water-filling* solution. Implementation of this scheme on a time-varying channel requires however continuous rate adaptation and is not feasible in any practical such system. In this paper, we show how to maximise the average spectral efficiency (ASE) of dual-branch MIMO systems (either two transmit or two receive antennas) with perfect transmitter and receiver CSI when using a fixed number of codes (discrete rate adaptation), and subsequently compare the resulting maximum ASE to the system's ergodic capacity. We assume that capacity-achieving codes for AWGN channels are available, and that the power available to the transmitter for transmitting the i th symbol frame is fixed and independent of the frame index i .

I. INTRODUCTION

Information theoretic results on the capacity of MIMO systems with both transmitter and receiver channel state information (CSI) suggest decoupling such channels into independent subchannels by means of linear precoding, and distributing the available power between these subchannels according to the *water-filling* solution [1]–[3]. Communication based on this scheme on a time-varying channel requires however continuous rate adaptation (i.e. the ability to implement any rate within the continuum covered by the statistical distribution of the channel realisations), and is unfortunately not feasible in a practical system. Indeed, although it is realistic to assume that capacity-achieving codes for AWGN channels of any desired rate can be designed thanks to advances in coding theory (concerning mainly turbo codes [4] and low-density parity-check codes [5]), only a finite number of such codes – and thus rates – will be available in any practical system due to memory and complexity constraints.

In this paper, we consider dual-branch MIMO systems (either two transmit or two receive antennas) in which the CSI is perfectly known to both the transmitter and the receiver, and a given finite number n_c of capacity-achieving codes for AWGN channels of different rates are available for use. We first show how to calculate the system's average spectral efficiency (ASE) (measured in bits per channel use) when the rates of these codes are fixed and the available power is optimally distributed between the different subchannels. Subsequently, we discuss how to optimally select the rates of these n_c codes in order to maximise the system's ASE, and compare the resulting maximum ASE – for values of n_c ranging from one to four – to the MIMO system's ergodic capacity.

We will assume for simplicity an i.i.d. MIMO Rayleigh flat-fading channel [2], [6], although we will see that our methodology is general and can be applied to other MIMO channel models as well. We also assume that the power available to the transmitter for the transmission of any given symbol frame is fixed and independent of the symbol frame in question. (In this paper, a symbol frame consists of a finite number of symbol vectors which are transmitted sequentially.)

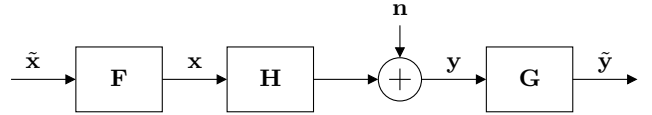


Fig. 1. MIMO System Model

II. SYSTEM MODEL

Let us consider a MIMO link with linear precoding and decoding [3] using N transmitting and M receiving antennas (see Fig. 1). We set $m \triangleq \min\{M, N\}$ and $n \triangleq \max\{M, N\}$. Assuming frequency-flat fading, such a MIMO link can be modelled in the complex baseband domain by the expression

$$\tilde{\mathbf{y}} = \mathbf{G}\mathbf{H}\mathbf{F}\tilde{\mathbf{x}} + \mathbf{G}\mathbf{n}, \quad (1)$$

where $\tilde{\mathbf{x}} \in \mathbb{C}^{m \times 1}$ represents the transmitted symbol vector, $\mathbf{H} \in \mathbb{C}^{M \times N}$ is the MIMO channel matrix, assumed to consist of i.i.d. Gaussian entries with independent, variance $1/2$ real and imaginary parts (modelling a Rayleigh-fading environment), $\mathbf{n} \in \mathbb{C}^{M \times 1}$ is a zero-mean circularly symmetric complex Gaussian noise vector with independent, equal variance real and imaginary parts, $\tilde{\mathbf{y}} \in \mathbb{C}^{m \times 1}$ is the receiver estimate for $\tilde{\mathbf{x}}$, and $\mathbf{F} \in \mathbb{C}^{N \times m}$, $\mathbf{G} \in \mathbb{C}^{m \times M}$ respectively represent the linear precoder and decoder matrices. We assume that the channel matrix \mathbf{H} remains constant during the transmission of all the symbol vectors in any given symbol frame, but that the channel matrices corresponding to different symbol frames are mutually independent and identically distributed (this corresponds to an i.i.d. block-fading channel). In addition, $\mathbf{x} \in \mathbb{C}^{N \times 1}$ and $\mathbf{y} \in \mathbb{C}^{M \times 1}$ appearing in Fig. 1 respectively denote the vector that is transmitted over the N -antenna array and the vector that is received by the M -antenna array. We assume $E[\tilde{\mathbf{x}}\tilde{\mathbf{x}}^\dagger] = I_{m \times m}$, $E[\mathbf{n}\mathbf{n}^\dagger] = I_{M \times M}$, and $E[\tilde{\mathbf{x}}\mathbf{n}^\dagger] = \mathbf{0}_{m \times M}$, where † denotes conjugate transposition (for simplicity we assume uncorrelated input sources, each normalised to unit power). For future use, we also define

$$\mathbf{W} = \begin{cases} \mathbf{H}^\dagger\mathbf{H} & \text{if } N \leq M, \text{ and} \\ \mathbf{H}\mathbf{H}^\dagger & \text{if } N > M. \end{cases} \quad (2)$$

Now, denote the singular value decomposition of the channel matrix \mathbf{H} by

$$\mathbf{H} = \mathbf{U}\mathbf{\Lambda}\mathbf{V}^\dagger, \quad (3)$$

where $\mathbf{U} \in \mathbb{C}^{M \times M}$ and $\mathbf{V} \in \mathbb{C}^{N \times N}$ are unitary matrices, and $\mathbf{\Lambda} \in \mathbb{R}^{M \times N}$ is a matrix having the nonnegative square roots of the eigenvalues $\lambda_1, \dots, \lambda_m$ of \mathbf{W} as entries on its main diagonal, and zeros elsewhere.

Setting $\mathbf{F} = \mathbf{V}\mathbf{\Phi}_f$ and $\mathbf{G} = \mathbf{\Phi}_g\mathbf{V}^\dagger\mathbf{H}^\dagger$, where $\mathbf{\Phi}_g \in \mathbb{R}^{m \times N}$ is such that¹

$$(\mathbf{\Phi}_g)_{i,j} = \begin{cases} 0 & \text{if } i \neq j \\ \phi_{g,i} & \text{if } i = j, \end{cases} \quad (4)$$

¹We use the notation $(\cdot)_{i,j}$ to denote the element in position (i, j) of the matrix in the argument.

with entries $\phi_{g,1}, \dots, \phi_{g,m}$ chosen arbitrarily under the constraint that Φ_g be of full rank, and $\Phi_f \in \mathbb{R}^{N \times m}$ also has the structure in (4) and entries $\phi_{f,1}, \dots, \phi_{f,m}$, it can be seen that (1) becomes

$$\tilde{\mathbf{y}} = \Phi_g \mathbf{\Lambda}^\dagger \mathbf{\Lambda} \Phi_f \tilde{\mathbf{x}} + \tilde{\mathbf{n}}, \quad (5)$$

where $\tilde{\mathbf{n}} \triangleq \mathbf{G}\mathbf{n}$. The MIMO link has thus been decoupled into m parallel, independent subchannels. For a given symbol frame (and corresponding channel matrix \mathbf{H}), the SNR γ_k on subchannel $k \in \{1, \dots, m\}$ is then given by [7]

$$\gamma_k = \frac{E[(\Phi_g \mathbf{\Lambda}^\dagger \mathbf{\Lambda} \Phi_f \tilde{\mathbf{x}})(\Phi_g \mathbf{\Lambda}^\dagger \mathbf{\Lambda} \Phi_f \tilde{\mathbf{x}})^\dagger]_{k,k}}{E[\tilde{\mathbf{n}}\tilde{\mathbf{n}}^\dagger]_{k,k}} = \lambda_k \phi_{f,k}^2. \quad (6)$$

We assume in addition that the transmitter must respect the power constraint²

$$E[\mathbf{x}^\dagger \mathbf{x}] = \text{tr}\{E[\mathbf{x}\mathbf{x}^\dagger]\} \leq P \quad (7)$$

during the transmission of every symbol frame, P being the total power budget. This can also be written

$$\text{tr}(\mathbf{F}\mathbf{F}^\dagger) = \sum_{k=1}^m \phi_{f,k}^2 \leq P. \quad (8)$$

$\phi_{f,k}^2$ is thus the power that is allocated to subchannel $k \in \{1, \dots, m\}$.

We conclude this section by remembering that the joint probability density of the ordered eigenvalues ($\lambda_1 \geq \dots \geq \lambda_m \geq 0$) of matrix \mathbf{W} is given in the case of i.i.d. Rayleigh fading by [6]

$$f_{\lambda_1, \dots, \lambda_m}(\lambda_1, \dots, \lambda_m) = K_{m,n}^{-1} e^{-\sum_{i=1}^m \lambda_i} \prod_{i=1}^m \lambda_i^{n-m} \prod_{\substack{i < j \\ 1 \leq i, j \leq m}} (\lambda_i - \lambda_j)^2, \quad (9)$$

where $K_{m,n}^{-1}$ is a normalising factor.³ This result will be used later in this document.

III. SYSTEM CAPACITY

For a given channel realisation \mathbf{H} , in order to maximise the information rate of the system described in Sec. II, it can be shown by information theoretic considerations that $\phi_{f,1}, \dots, \phi_{f,m}$ should satisfy [1], [7]

$$\phi_{f,k}^2 = (\mu - \lambda_k^{-1})_+ \quad \forall k \in \{1, \dots, m\}, \quad (10)$$

where $(\cdot)_+ \triangleq \max(\cdot, 0)$ and μ is a constant which is set by the power constraint given in (8). This is the well-known *water-filling* solution. Attaining this maximum information rate (or *capacity C*) however requires continuous rate adaptation: denoting by γ_k the SNR resulting on the k th subchannel after distributing the available power according to (10), it can be seen that – for each symbol frame and each one of the k among m subchannels – a capacity achieving code designed to operate at the information rate $\log_2(1 + \gamma_k)$ on an AWGN channel has to be utilised. Since the subchannel SNR distributions $f_{\gamma_1}(\gamma_1), \dots, f_{\gamma_m}(\gamma_m)$ have a continuous component [8], an infinite number of such capacity-achieving-codes is required if we are to cover all possible channel realisations.

The system ergodic capacity C is given by the sum of the capacities of each one of the m subchannels, namely

$$C = \sum_{k=1}^m \int_0^\infty \log_2(1 + \gamma_k) f_{\gamma_k}(\gamma_k) d\gamma_k, \quad [\text{bits/channel use}] \quad (11)$$

where the capacity of each subchannel is calculated as in [9, eq. (2)]. Expressions for the subchannel SNR distributions $f_{\gamma_k}(\gamma_k)$ were derived in [8] for the case of Rayleigh-fading dual-branch MIMO systems.

²In future research, we plan to consider a per-antenna power constraint.

³We have $K_{2,n} = (n-1)!(n-2)!$ when $m = 2$.

IV. MAXIMUM ASE OF DISCRETE-RATE DUAL-BRANCH MIMO SYSTEMS

In the case of discrete-rate adaptation, only a finite number n_c of capacity-achieving codes for AWGN channels is available for use. In this section, we first show how to calculate the ASE of a dual-branch MIMO system when the rates $\{R_i\}_{i=1}^{n_c}$ of these n_c codes are fixed and the available power P is optimally distributed between the $m = 2$ subchannels. We then discuss how to find the values $\{R_{n_c}^*\}_{i=1}^{n_c}$ of the rates for which such a system's ASE is maximised.

A. Optimal power allocation and ASE calculation for fixed R_{n_c}, \dots, R_1

Let us define the *rate vector* $\mathbf{R}_{n_c} \triangleq (R_{n_c}, \dots, R_1, R_0 = 0)$ (we set $R_0 = 0$ for convenience although R_0 is not an optimisation variable), the *power allocation vector* $\mathbf{P}_m \triangleq (\phi_{f,1}^2, \dots, \phi_{f,m}^2)$, and the *vector of eigenvalues* $\mathbf{L}_m \triangleq (\lambda_1, \dots, \lambda_m)$. All these will be potentially different for every realisation of the channel matrix \mathbf{H} . Now, for any given \mathbf{R}_{n_c} , \mathbf{L}_m , and \mathbf{P}_m , we define the *instantaneous information rate* $\nu(\mathbf{R}_{n_c}, \mathbf{L}_m, \mathbf{P}_m)$ by

$$\nu(\mathbf{R}_{n_c}, \mathbf{L}_m, \mathbf{P}_m) \triangleq \sum_{k=1}^m \log_2(1 + \lambda_k \phi_{f,k}^2), \quad (12)$$

where the power constraint $\sum_{k=1}^m \phi_{f,k}^2 \leq P$, and the rate constraints $\log_2(1 + \lambda_k \phi_{f,k}^2) \in \mathbf{R}_{n_c} \forall k \in \{1, \dots, m\}$, must be satisfied in order for \mathbf{P}_m to be a valid power allocation vector.

For any given \mathbf{R}_{n_c} and \mathbf{L}_m , the optimal power allocation vector $\mathbf{P}_m^* \triangleq (\phi_{f,1}^{*2}, \dots, \phi_{f,m}^{*2})$ is given by

$$\mathbf{P}_m^* = \arg \max_{\mathbf{P}_m} \nu(\mathbf{R}_{n_c}, \mathbf{L}_m, \mathbf{P}_m), \quad (13)$$

where the power and rate constraints mentioned above must obviously still be satisfied. For fixed \mathbf{R}_{n_c} , the maximal ASE, $\eta(\mathbf{R}_{n_c})$, is then simply given by

$$\eta(\mathbf{R}_{n_c}) = \int_{\Omega_m} \nu(\mathbf{R}_{n_c}, \mathbf{L}_m, \mathbf{P}_m^*) f_{\lambda_1, \dots, \lambda_m}(\lambda_1, \dots, \lambda_m) d\Lambda_m, \quad (14)$$

where $\Omega_m \triangleq \{(\lambda_1, \dots, \lambda_m) | \lambda_1 \geq \dots \geq \lambda_m \geq 0\} \subset \mathbb{R}^m$, $d\Lambda_m \triangleq d\lambda_m \dots d\lambda_1$, and $f_{\lambda_1, \dots, \lambda_m}(\lambda_1, \dots, \lambda_m)$ was defined in (9). For convenience, we also define

$$\nu^*(\mathbf{R}_{n_c}, \mathbf{L}_m) \triangleq \nu(\mathbf{R}_{n_c}, \mathbf{L}_m, \mathbf{P}_m^*). \quad (15)$$

In the remainder of this section, we show how to calculate the ASE $\eta(\mathbf{R}_{n_c})$ for dual-branch MIMO systems ($m = 2$) and $n_c \in \{1, 2, 3, 4\}$. We assume without loss of generality that $R_{n_c} > \dots > R_1 > R_0 = 0$. (If, in the previous relation, the strict inequalities were to be replaced with non-strict inequalities, the results of this section would still apply. However, in this case it is obvious that whenever \mathbf{R}_{n_c} is such that k of these non-strict inequalities are satisfied with equality, the calculation of $\eta(\mathbf{R}_{n_c})$ can be reduced to that of $\eta(\mathbf{R}'_{n_c-k})$, where \mathbf{R}'_{n_c-k} is obtained from \mathbf{R}_{n_c} by removing any repeated components and renumbering.)

We first calculate $\nu^*(\mathbf{R}_{n_c}, \mathbf{L}_2)$ and then obtain $\eta(\mathbf{R}_{n_c})$ via (14). For $i \in \{0, \dots, n_c\}$, let $\gamma_i^* \triangleq 2^{R_i} - 1$, and let

$$A_{ij} \triangleq \left\{ (\lambda_1, \lambda_2) \in \Omega_2 \left| \frac{\gamma_i^*}{\lambda_1} + \frac{\gamma_j^*}{\lambda_2} \leq P \right. \right\}, \quad (16)$$

where $i \in \{0, \dots, n_c\}$ and $j \in \{0, \dots, i\}$. We also define

$$r(A_{ij}) \triangleq R_i + R_j \quad (17)$$

for each A_{ij} . For every set F of points of Ω_2 , we can consider the event “observing a channel matrix \mathbf{H} such that the corresponding $(\lambda_1, \lambda_2) \in F$ ”. The probability that this event take place is given by

$$\Pr(F) = \int_F f(\lambda_1, \lambda_2) d\lambda_2 d\lambda_1, \quad (18)$$

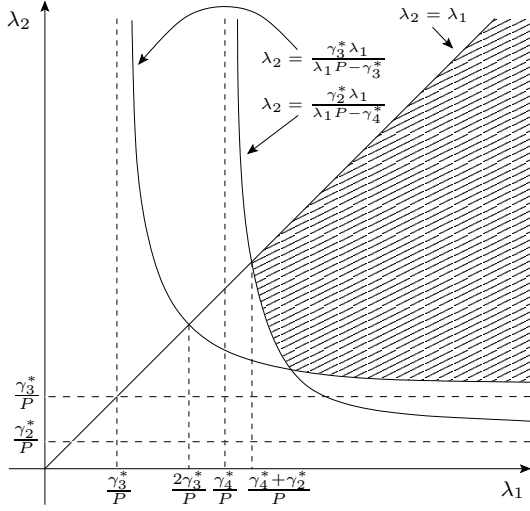


Fig. 2. Calculation of $\Pr(A_{42} \cap A_{33})$ using (19). The shaded area corresponds to $\{(\lambda_1, \lambda_2) \in A_{42} \cap A_{33}\}$.

where we have chosen to use the same letter for the set of points of Ω_2 and the event defined by this set, the meaning being clear from the context. For simplicity, we refer to this quantity as the *probability of set F*. It is important at this point to note that the probability of any finite intersection of the form $I = \bigcap_k A_{i_k j_k}$ can be easily obtained as

$$\Pr(I) = \int_{\max_k \xi_k}^{\infty} \int_{\max_k \eta_k}^{\lambda_1} f(\lambda_1, \lambda_2) d\lambda_2 d\lambda_1, \quad (19)$$

where $\xi_k = \frac{\gamma_{i_k}^* + \gamma_{j_k}^*}{P}$ and $\eta_k = \frac{\gamma_{j_k}^* \lambda_1}{\lambda_1^P - \gamma_{i_k}^*}$. This is illustrated in Fig. 2 for $I = A_{42} \cap A_{33}$, where the shaded area corresponds to $\{(\lambda_1, \lambda_2) \in A_{42} \cap A_{33}\}$. Furthermore, we can use mathematical induction to prove that

$$\begin{aligned} \Pr\left(F \setminus \bigcup_{k=1}^{\kappa} F_k\right) &= \Pr(F) - \sum_{k=1}^{\kappa} \Pr(F \cap F_k) \\ &+ \sum_{k,l | k < l} \Pr(F \cap F_k \cap F_l) + \dots \\ &+ (-1)^{\kappa} \Pr\left(F \cap \bigcap_{k=1}^{\kappa} F_k\right). \end{aligned} \quad (20)$$

This identity allows us to evaluate any expression of the form $\Pr(I \setminus J)$, with I defined as above and J a finite union of the form $J = \bigcup_l A_{i_l j_l}$. Indeed, each one of the terms in the expression which is obtained by applying (20) to $\Pr(I \setminus J)$ is a finite intersection of $A_{i_j s}$ which can be computed using (19). We now separately consider the cases $n_c = 1$ and $n_c \in \{2, 3, 4\}$.

1) $n_c = 1$: In this case, we have a single code of rate R_1 . For a given channel matrix \mathbf{H} and corresponding λ_1 and λ_2 , $\nu^*(\mathbf{R}_1, \mathbf{L}_2)$ will be equal to $2R_1$ if the power budget is large enough to support a code of rate R_1 on both subchannels, i.e. if

$$\begin{cases} \frac{\gamma_1^*}{\lambda_1} \leq P \\ \frac{\gamma_2^*}{\lambda_2} \leq P \\ \frac{\gamma_1^*}{\lambda_1} + \frac{\gamma_2^*}{\lambda_2} \leq P. \end{cases} \quad (21)$$

The first and second inequalities respectively state that the available power must be sufficient to support a rate R_1 on the first (best) and second (worst) subchannels. The third inequality states that the sum of the powers that is allocated to both subchannels must not exceed the total available power P . Since $\lambda_1 \geq \lambda_2 \geq 0$, it can easily be seen that

the first inequality is automatically verified if the second is, and that the first two are whenever the third is. Consequently, if $\frac{\gamma_1^*}{\lambda_1} + \frac{\gamma_2^*}{\lambda_2} \leq P$, i.e. if $(\lambda_1, \lambda_2) \in A_{11}$, the optimal power distribution is characterised by $\phi_{f,k}^{*2} = \frac{\gamma_k^*}{\lambda_k}$ ($k = 1, 2$), and $\nu^*(\mathbf{R}_1, \mathbf{L}_2) = r(A_{11}) = 2R_1$.

If λ_1 and λ_2 are such that – given the available power budget P – only one subchannel can support transmission at a rate R_1 , we will have $\nu^*(\mathbf{R}_1, \mathbf{L}_2) = R_1$. It can be verified that this happens if and only if

$$\begin{cases} \frac{\gamma_1^*}{\lambda_1} \leq P \\ \frac{\gamma_1^*}{\lambda_1} + \frac{\gamma_2^*}{\lambda_2} > P, \end{cases} \quad (22)$$

i.e. if $(\lambda_1, \lambda_2) \in A_{10} \setminus A_{11}$. Finally, $\nu^*(\mathbf{R}_1, \mathbf{L}_2) = 0$ if none of the subchannels can support transmission at a rate R_1 , which is the case if $\frac{\gamma_1^*}{\lambda_1} > P$, i.e. if $(\lambda_1, \lambda_2) \in \Omega_2 \setminus A_{10}$.

Bearing in mind the above results, $\eta(\mathbf{R}_1)$ can be calculated using (14). This yields

$$\eta(\mathbf{R}_1) = r(A_{11}) \cdot \Pr(A_{11}) + r(A_{10}) \cdot \Pr(A_{10} \setminus A_{11}), \quad (23)$$

where $\Pr(A_{11})$ and $\Pr(A_{10} \setminus A_{11})$ can be found using (19) and (20).

2) $n_c = 2$, $n_c = 3$, and $n_c = 4$: Proceeding exactly as in the case $n_c = 1$, it is possible to derive expressions for $\eta(\mathbf{R}_2)$, $\eta(\mathbf{R}_3)$, and $\eta(\mathbf{R}_4)$. (The details are somewhat tedious and not included here.) This yields

$$\eta(\mathbf{R}_{n_c}) = \sum_{k=1}^{2(2^{n_c}-1)} S_{n_c,k} \cdot T_{n_c,k}, \quad n_c \in \{2, 3, 4\}. \quad (24)$$

Expressions for $S_{4,k}$ and $T_{4,k}$ are given in Table I. (The corresponding tables for $n_c \in \{2, 3\}$ are not included here due to space requirements.) Note that $T_{4,k}$ can be computed using (19) and (20) for $k \in \{1, \dots, 30\}$ (this is also the case for $T_{2,k}$ and $T_{3,k}$). It is also interesting to remember that the expression for $\eta(\mathbf{R}_4)$ given in (24) can be used to compute $\eta(\mathbf{R}_1)$, $\eta(\mathbf{R}_2)$, and $\eta(\mathbf{R}_3)$. Indeed, we have e.g. $\eta((x, y, 0, 0, 0)) = \eta((x, y, 0))$ for all $x > y > 0$.

Note that the methodology presented in this section can also be used to evaluate $\eta(\mathbf{R}_{n_c})$ for other dual-branch MIMO channel models (e.g. correlated MIMO Rayleigh-fading channels [10] or Ricean fading channels [11]) simply by using the appropriate expression for the eigenvalue distribution $f_{\lambda_1, \lambda_2}(\lambda_1, \lambda_2)$ in (19).

B. Maximising the ASE with respect to the component rates

In this section, we discuss how to find the rate vector $\mathbf{R}_{n_c}^* = \arg \max_{\mathbf{R}_{n_c}} \eta(\mathbf{R}_{n_c})$ resulting in the maximum ASE $\eta(\mathbf{R}_{n_c}^*)$ when $n_c \in \{1, 2, 3, 4\}$. (Note that for every \mathbf{L}_m , the values of $\mathbf{R}_{n_c}^*$ and \mathbf{P}_m^* – the latter quantity being obtained via eq. (13) with $\mathbf{R}_{n_c} = \mathbf{R}_{n_c}^*$ – will be *jointly* optimal. However, whereas $\mathbf{R}_{n_c}^*$ remains fixed, the value of \mathbf{P}_m^* changes as a function of \mathbf{L}_m .) This is an n_c -dimensional optimisation problem. The most straightforward approach to solve it would be to compute the points where the gradient $\nabla_{\mathbf{R}_{n_c}} \eta(\mathbf{R}_{n_c})$ vanishes. It is unfortunately not practical to do this analytically since the expressions for $\eta(\mathbf{R}_{n_c})$ are quite involved for all values of $n_c \in \{1, 2, 3, 4\}$.

A plot of $\eta(\mathbf{R}_1)$ as a function of R_1 reveals that this function can have several local maxima (see Fig. 3(a)). Further numerical experiments reveal that the total number of local maxima increases rapidly with n_c . It is thus necessary to explore the whole n_c -dimensional space to find the optimal \mathbf{R}_{n_c} . When $n_c = 1$ or $n_c = 2$ this can be done by plotting $\eta(\mathbf{R}_{n_c})$ as a function of (R_{n_c}, \dots, R_1) for $M_{n_c} > R_{n_c} > \dots > R_1 > 0$, where M_{n_c} is a suitably chosen number whose value serves to limit the search space. (How to choose M_{n_c} is discussed in the Appendix.) The approximate positions of all the local maxima then become apparent, and it is possible to find the value of $\eta(\mathbf{R}_{n_c}^*)$ at each local maximum by using a steepest-descent like algorithm [12] with a starting point sufficiently close to the local

k	$S_{4,k}$	$T_{4,k}$
1	$r(A_{44})$	$\Pr(A_{44})$
2	$r(A_{43})$	$\Pr(A_{43} \setminus A_{44})$
3	$r(A_{42})$	$\Pr(A_{42} \setminus A_{43})$
4	$r(A_{41})$	$\Pr(A_{41} \setminus A_{42})$
5	$r(A_{40})$	$\Pr(A_{40} \setminus A_{41})$
6	$r(A_{33})$	$\Pr(A_{33} \setminus A_{40})$
7	$r(A_{32})$	$\Pr(A_{32} \setminus (A_{33} \cup A_{40}))$
8	$r(A_{31})$	$\Pr(A_{31} \setminus (A_{22} \cup A_{40}))$
9	$r(A_{30})$	$\Pr(A_{30} \setminus (A_{11} \cup A_{40}))$
10	$r(A_{22})$	$\Pr(A_{22} \setminus A_{30})$
11	$r(A_{21})$	$\Pr(A_{21} \setminus (A_{22} \cup A_{30}))$
12	$r(A_{20})$	$\Pr(A_{20} \setminus (A_{11} \cup A_{30}))$
13	$r(A_{11})$	$\Pr(A_{11} \setminus A_{20})$
14	$r(A_{10})$	$\Pr(A_{10} \setminus (A_{11} \cup A_{20}))$
15	$\max\{r(A_{33}), r(A_{42})\}$	$\Pr((A_{33} \cap A_{42}) \setminus A_{43})$
16	$\max\{r(A_{33}), r(A_{41})\}$	$\Pr((A_{33} \cap A_{41}) \setminus A_{42})$
17	$\max\{r(A_{33}), r(A_{40})\}$	$\Pr((A_{33} \cap A_{40}) \setminus A_{41})$
18	$\max\{r(A_{32}), r(A_{41})\}$	$\Pr((A_{32} \cap A_{41}) \setminus (A_{33} \cup A_{42}))$
19	$\max\{r(A_{32}), r(A_{40})\}$	$\Pr((A_{32} \cap A_{40}) \setminus (A_{33} \cup A_{41}))$
20	$\max\{r(A_{31}), r(A_{40}), r(A_{22})\}$	$\Pr((A_{31} \cap A_{40} \cap A_{22}) \setminus (A_{32} \cup A_{41}))$
21	$\max\{r(A_{40}), r(A_{22})\}$	$\Pr((A_{40} \cap A_{22}) \setminus A_{31})$
22	$\max\{r(A_{31}), r(A_{40})\}$	$\Pr((A_{31} \cap A_{40}) \setminus (A_{22} \cup A_{41}))$
23	$\max\{r(A_{22}), r(A_{41})\}$	$\Pr((A_{41} \cap A_{22}) \setminus A_{32})$
24	$\max\{r(A_{22}), r(A_{31})\}$	$\Pr((A_{22} \cap A_{31}) \setminus (A_{32} \cup A_{40}))$
25	$\max\{r(A_{22}), r(A_{30})\}$	$\Pr((A_{22} \cap A_{30}) \setminus (A_{31} \cup A_{40}))$
26	$\max\{r(A_{21}), r(A_{40})\}$	$\Pr((A_{21} \cap A_{40}) \setminus (A_{31} \cup A_{22}))$
27	$\max\{r(A_{21}), r(A_{30})\}$	$\Pr((A_{21} \cap A_{30}) \setminus (A_{31} \cup A_{40} \cup A_{22}))$
28	$\max\{r(A_{11}), r(A_{40})\}$	$\Pr((A_{11} \cap A_{40}) \setminus A_{21})$
29	$\max\{r(A_{11}), r(A_{30})\}$	$\Pr((A_{11} \cap A_{30}) \setminus (A_{21} \cup A_{40}))$
30	$\max\{r(A_{11}), r(A_{20})\}$	$\Pr((A_{11} \cap A_{20}) \setminus (A_{21} \cup A_{30}))$

TABLE I
EXPRESSIONS FOR $S_{4,k}$ AND $T_{4,k}$

maximum in question. The values of $\mathbf{R}_{n_c}^*$ and $\eta(\mathbf{R}_{n_c}^*)$ immediately follow.

When $n_c \geq 3$, it becomes more difficult to plot $\eta(\mathbf{R}_{n_c})$ as a function of $\{R_i\}_{i=1}^{n_c}$ for $M_{n_c} > R_{n_c} > \dots > R_1 > 0$. We therefore proceed by evaluating $\eta(\mathbf{R}_{n_c})$ at all points of the form $(i_{n_c} \cdot \Delta, \dots, i_1 \cdot \Delta)$, where $i_{n_c} > \dots > i_1 > 0$ are whole numbers, $(i_{n_c} + 1) \cdot \Delta > M_{n_c} > i_{n_c} \cdot \Delta$, and Δ is a suitably chosen quantity (see Sec. V).⁴ The resulting values can then be sorted, and a steepest-descent like algorithm can be used (starting from each one of the rate vectors \mathbf{R}_{n_c} resulting in one of the top N_p ASE values $\eta(\mathbf{R}_{n_c})$) to attempt to find the local maxima which are in the neighbourhood of each one of these N_p points, where N_p is a sufficiently large integer (see Sec. V). One of the local maxima obtained in this way will then hopefully be the global maximum, although rigorously proving this is difficult and beyond the scope of this paper. The results presented in Sec. V can thus be considered as lower bounds for the maximum ASE $\eta(\mathbf{R}_{n_c}^*)$ when $n_c = 3$ and $n_c = 4$.

We conclude this section with some additional remarks regarding the maximisation of $\eta(\mathbf{R}_{n_c})$. Note first of all (see table I) that due to the presence of terms of the form $\max_l \{r(A_{i_l j_l})\}$ in the expression for $S_{n_c, k}$, $\eta(\mathbf{R}_{n_c})$ is not differentiable at all points $\mathbf{R}_{n_c} \in \mathcal{R}_{n_c}^\circ$ when $n_c = 4$, where $\mathcal{R}_{n_c}^\circ$ denotes the interior of the set $\mathcal{R}_{n_c} \triangleq \{(R_{n_c}, \dots, R_1, 0) | M_{n_c} > R_{n_c} > \dots > R_1 > 0\}$ (this turns out to be the case also when $n_c \in \{2, 3\}$). Strictly speaking, this precludes the use of steepest-descent like algorithms to maximise $\eta(\mathbf{R}_{n_c})$. To avoid this problem, one can for example consider writing $\mathcal{R}_{n_c} = \bigcup_l \mathcal{R}_{n_c, l}$, where $\mathcal{R}_{n_c, k}^\circ \cap \mathcal{R}_{n_c, l}^\circ = \emptyset$ for all $k \neq l$ and $\eta(\mathbf{R}_{n_c})$ is differentiable on $\mathcal{R}_{n_c, l}^\circ$ for all l . Constrained optimisation algorithms can then be used to maximise $\eta(\mathbf{R}_{n_c})$ on $\mathcal{R}_{n_c, l}$ for all l . It can however be verified that when $n_c = 4$, at least 286 different such

⁴Genetic algorithms provide an interesting alternative which hasn't been explored by the authors in this context [13].

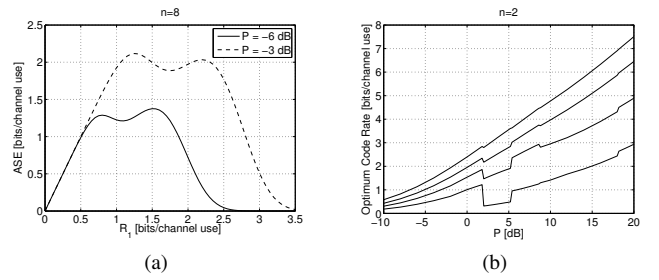


Fig. 3. Fig. 3(a) shows the ASE $\eta(\mathbf{R}_1)$ as a function of R_1 for $n = 8$ and $P = -6$ dB (solid curve) and for $n = 8$ and $P = -3$ dB (dashed curve). In Fig 3(b), the calculated code rates $\{\hat{R}_i^*\}_{i=1}^4$, which (approximately) maximise $\eta(\mathbf{R}_4)$, are plotted as a function of the power budget P for $n = 2$.

sets are required, and that this number rapidly increases with n_c . Furthermore, numerical simulations show that $\eta(\mathbf{R}_{n_c})$ can have more than one local maximum on some of these sets. This approach was thus considered impractical and not followed here.

Another possibility is to use optimisation algorithms which do not require that the function to be optimised be differentiable, like for example the Nelder-Mead simplex algorithm [14]. Nevertheless, numerical simulations show that in practise good results can be obtained by simply ignoring this problem and using steepest-descent like algorithms as described above, which is the approach that was followed here.

We would also like to point the reader's attention to the fact that although the ASE computation as presented in Sec. IV-A can be extended without too much difficulty to $n_c > 4$, the problem of finding $\mathbf{R}_{n_c}^*$ and $\eta(\mathbf{R}_{n_c}^*)$ becomes increasingly complex and quickly becomes intractable. However, the results from Sec. V show that for when $n_c = 4$ and $P < 20$ dB, the maximum attainable ASE is within 1 dB of the ergodic capacity for $n = 2$, and within less than 0.5 dB of the ergodic capacity when $n = 8$. The gain that can be achieved by increasing the value of n_c is thus small.

V. NUMERICAL RESULTS

We use the notation $\hat{\mathbf{R}}_{n_c}^*$ for the approximation for $\mathbf{R}_{n_c}^*$ obtained by numerical simulations when $n_c \in \{3, 4\}$. We also find it convenient to introduce

$$\tilde{\mathbf{R}}_{n_c}^* = \begin{cases} \mathbf{R}_{n_c}^* & \text{if } n_c \in \{1, 2\} \\ \hat{\mathbf{R}}_{n_c}^* & \text{if } n_c \in \{3, 4\}. \end{cases} \quad (25)$$

We calculated the ergodic capacity C (given in eq. (11)), and the value of $\eta(\tilde{\mathbf{R}}_{n_c}^*)$ (together with the corresponding vector $\tilde{\mathbf{R}}_{n_c}^*$) using the method described in Sec. IV. Numerical integration algorithms were used whenever required (e.g. to evaluate integrals of the form (19) and the integrals appearing in (11)), and routines from the CFSQP source code [15] were used to find the local maxima of $\eta(\mathbf{R}_{n_c})$. This was done for $n_c \in \{1, 2, 3, 4\}$, $m = 2$ (dual-branch MIMO systems), $n \in \{2, 4, 8\}$ and a power budget $P \in [-10 \text{ dB}, 20 \text{ dB}]$. When computing $\eta(\hat{\mathbf{R}}_{n_c}^*)$ for $n_c \in \{3, 4\}$, we set $\Delta = M_{n_c}/22$ to keep computational complexity at an acceptable level. (For each value of P and n , this corresponds to 9109 evaluations of $\eta(\mathbf{R}_4)$ and to 1794 evaluations of $\eta(\mathbf{R}_3)$.) We also set $N_p = 500$ when $n_c = 4$, and $N_p = 100$ when $n_c = 3$.

The effect of the presence of several local maxima in $\eta(\mathbf{R}_{n_c})$ is illustrated in Fig. 3. Fig. 3(a) shows the ASE $\eta(\mathbf{R}_1)$ as a function of R_1 for $n = 8$ and $P = -6$ dB, and for $n = 8$ and $P = -3$ dB. There are two distinct local maxima, and it can be seen that when $P = -6$ dB the global maximum is situated at the local maximum with the largest value of R_1 , whereas it is situated at the local maximum with the smallest value of R_1 when $P = -3$ dB. This creates a discontinuity in the value of R_1^* maximising $\eta(\mathbf{R}_1)$ as P increases

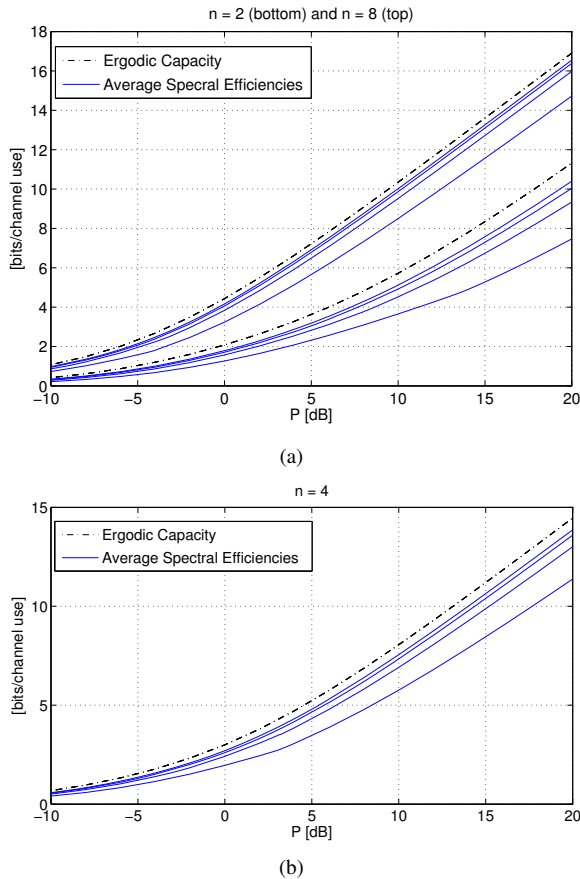


Fig. 4. The figures show – for $n = 2$ (a, bottom), $n = 8$ (a, top), and $n = 4$ (b) – the system capacity and the ASEs $\eta(\mathbf{R}_{n_c}^*)$ for $n_c = 1, n_c = 2, n_c = 3$, and $n_c = 4$ (bottom to top) as a function of the power budget P .

from -6 dB to -3 dB, although $\eta(\mathbf{R}_1^*)$ itself remains continuous. Such discontinuities are illustrated in Fig. 3(b) for $n = 2$ and $n_c = 4$.

The system's ergodic capacity and ASEs $\eta(\mathbf{R}_{n_c}^*)$ for $n_c = 1, n_c = 2, n_c = 3$, and $n_c = 4$ are shown in Fig. 4(a), for $n \in \{2, 8\}$, and in Fig. 4(b) for $n = 4$. As expected, $\eta(\mathbf{R}_{n_c}^*)$ approaches the system's ergodic capacity C as n_c increases. (Outage probability plots, and plots displaying the resulting power and rate distributions for selected values of $\mathbf{R}_{n_c}^*$ are not included here due to space requirements.) It is our belief that results such as those presented in Fig. 4 can be an extremely valuable tool when seeking to maximise the ASE during the design of MIMO communication systems.

VI. CONCLUSIONS

In this paper, we consider the problem of maximising the ASE of dual-branch MIMO systems with perfect transmitter and receiver CSI when using a fixed number of codes, assuming the availability of a finite number of capacity-achieving codes for AWGN channels and a fixed power constraint that the transmitter must respect during the transmission of every symbol frame. After showing how to calculate the system's ASE for fixed values of the rates of the available codes, we discuss how to optimally select these rates in order to maximise the system's ASE. The resulting maximum ASE (when using one, two, three, and four codes) is then compared to the MIMO system's ergodic capacity. It is the authors' belief that such results can be of great help in the design of MIMO systems.

APPENDIX

A value for M_{n_c} can for example be obtained as follows: let us assume that a lower bound η_{lb} for $\eta(\mathbf{R}_{n_c}^*)$ is known (such a

lower bound can for example be obtained by evaluating $\eta(\mathbf{R}_{n_c})$ for different values of \mathbf{R}_{n_c} , and that the value of $\eta(\mathbf{R}_{n_c-1}^*)$ is known as well. Let us define $g(R_{n_c}) \triangleq 2R_{n_c} \cdot \Pr(A_{n_c,0})$, where $\gamma_{n_c}^* = 2^{R_{n_c}} - 1$ in the definition of $A_{n_c,0}$ (see (16)), and let M_{n_c} be the largest value such that

$$\eta_{lb} = \eta(\mathbf{R}_{n_c-1}^*) + g(M_{n_c}), \quad (26)$$

which can be found by utilising numerical root-finding algorithms. It can be verified that $g(R_{n_c})$ decreases with increasing R_{n_c} for all $R_{n_c} > M_{n_c}$. Therefore, for all \mathbf{R}_{n_c} such that $R_{n_c} > M_{n_c}$, we have

$$\eta(\mathbf{R}_{n_c}) \leq \eta(\mathbf{R}_{n_c-1}^*) + g(R_{n_c}) < \eta_{lb}, \quad (27)$$

and hence we must have $R_{n_c} \leq M_{n_c}$ if η_{lb} is to be attained.

The first inequality in (27) follows from the following fact: noting that $(\lambda_1, \lambda_2) \in A_{n_c,0}$ if and only if event E – defined as “transmission at a rate R_{n_c} is done on at least one of the $m = 2$ subchannels” – takes place, we have

$$\begin{aligned} \eta(\mathbf{R}_{n_c}) &= \eta(\mathbf{R}_{n_c}|E)\Pr(E) + \eta(\mathbf{R}_{n_c}|\neg E)\Pr(\neg E) \\ &\leq \eta(\mathbf{R}_{n_c}|E)\Pr(E) + \eta(\mathbf{R}_{n_c}|\neg E)\Pr(\neg E) \\ &= \eta(\mathbf{R}_{n_c}|E)\Pr(A_{n_c,0}) + \eta(\mathbf{R}_{n_c}|\neg E)\Pr(\neg A_{n_c,0}) \\ &\leq \eta(\mathbf{R}_{n_c-1}^*) + 2R_{n_c} \cdot \Pr(A_{n_c,0}), \end{aligned} \quad (28)$$

where $\eta(\mathbf{R}_{n_c}|E)$ ($\eta(\mathbf{R}_{n_c}|\neg E)$) denotes the ASE when the rate vector is \mathbf{R}_{n_c} and event E takes (does not take) place, and $\Pr(E)$ ($\Pr(\neg E)$) denotes the probability that event E (not) take place.

REFERENCES

- [1] T. Cover and J. Thomas, *Elements of Information Theory*. John Wiley & Sons, 1991.
- [2] S. K. Jayaweera and H. V. Poor, “Capacity of multiple-antenna systems with both receiver and transmitter channel state information,” *IEEE Trans. Inform. Theory*, vol. 49, no. 10, pp. 2697–2709, Oct. 2003.
- [3] H. Sampath, P. Stoica, and A. Paulraj, “Generalized linear precoder and decoder design for MIMO channels using the weighted MMSE criterion,” *IEEE Trans. Commun.*, vol. 49, no. 12, pp. 2198–2206, Dec. 2001.
- [4] C. Berrou, A. Glavieux, and P. Thitimajshima, “Near Shannon limit error-correcting coding and decoding: Turbo-codes,” in *Proc. ICC International Conference on Communications, Geneva, Switzerland*, May 1993, pp. 1064–1070.
- [5] R. Gallager, “Low-density parity-check codes,” Ph.D. dissertation, MIT Press, Cambridge, MA, 1963.
- [6] E. Telatar, “Capacity of multi-antenna Gaussian channels,” AT&T Bell Laboratories, Tech. Rep., June 1995.
- [7] M. Kiessling, I. Viering, M. Reinhardt, and J. Speidel, “Short-term and long-term diagonalization of correlated MIMO channels with adaptive modulation,” in *Proc. IEEE International Symposium on Personal, Indoor and Mobile Radio Communications*, 2002, pp. 593–597.
- [8] S. de la Kethulle de Ryhove, G. E. Øien, and F. Bøghagen, “Subchannel SNR distributions in dual-branch MIMO systems,” in *Proc. IEEE/ITG Intern. Workshop on Smart Antennas*, (Duisburg, Germany), April 2005.
- [9] A. J. Goldsmith and P. P. Varaiya, “Capacity of fading channels with channel side information,” *IEEE Trans. Inform. Theory*, vol. 43, no. 6, pp. 1986–1992, Nov. 1997.
- [10] M. Chiani, M. Win, and A. Zanella, “On the capacity of spatially correlated MIMO Rayleigh-fading channels,” *IEEE Trans. Inform. Theory*, vol. 49, no. 10, pp. 2263–2371, Oct. 2003.
- [11] F. Bøghagen, P. Orten, and G. E. Øien, “On the Shannon capacity of dual MIMO systems in Ricean fading,” in *Proc. Vth IEEE Workshop on Signal Processing Advances in Wireless Communications (SPAWC)*, New York, June 2005, pp. 114–118.
- [12] J. Nocedal and S. J. Wright, *Numerical Optimization*. Springer Series in Operations Research, 1999.
- [13] D. Goldberg, *Genetic Algorithms in Search, Optimization, and Machine Learning*. Addison Wesley Publishing Company, 1989.
- [14] J. A. Nelder and R. Mead, “A simplex method for function minimization,” *The Computer Journal*, vol. 7, no. 4, pp. 308–313, 1965.
- [15] C. Lawrence, J. Zhou, and A. Tits, “User's guide for CFSQP version 2.5d.” AEM Design, Inc., 1997. [Online]. Available: <http://www.aemdesign.com/downloadfsqp.htm>